NANO LETTERS

Letter

pubs.acs.org/NanoLett

Raman Fingerprint of Aligned Graphene/h-BN Superlattices

Axel Eckmann,[†] Jaesung Park,[‡] Huafeng Yang,[†] Daniel Elias,[‡] Alexander S. Mayorov,[‡] Geliang Yu,[‡] Rashid Jalil,[‡] Kostya S. Novoselov,[‡] Roman V. Gorbachev,[‡] Michele Lazzeri,[§] Andre K. Geim,[‡] and Cinzia Casiraghi*[,†,∥]

[†]School of Chemistry and [‡]School of Physics and Astronomy, University of Manchester, Manchester, United Kingdom

[§]IMPMC, CNRS, Universite' Paris 6, Paris, France

[∥]Physics Department, Freie Universität Berlin, Berlin, Germany

Supporting Information

ABSTRACT: Graphene placed on hexagonal-boron nitride (h-BN) experiences a superlattice (Moiré) potential, which leads to a strong reconstruction of graphene's electronic spectrum with new Dirac points emerging at sub-eV energies. Here we study the effect of such superlattices on graphene's Raman spectrum. In particular, the 2D Raman peak is found to be exquisitely sensitive to the misalignment between graphene and h-BN lattices, probably due to the presence of a strain distribution with the same periodicity of the Moiré potential. This feature can be used to identify graphene superlattices with a misalignment angle smaller than 2°.

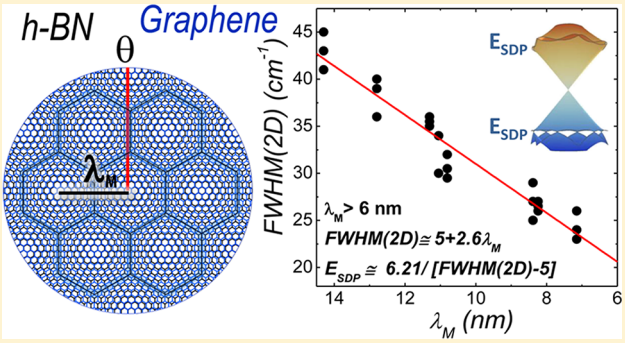

KEYWORDS: *Graphene, Raman spectroscopy, superlattice, boron nitride*

Periodic potentials universally result in spectral gaps at the Brillouin zone boundaries.[1] In the case of massless Dirac electrons, it has been shown theoretically and experimentally that a periodic potential leads to the formation of locally gapped regions (mini-gaps) characterized by superlattice Dirac points (SDPs), whose energy is determined by the wavelength of the potential.[2−7] Anisotropy of the Fermi velocity at the SDPs has been also predicted.[2] Therefore, one can modify graphene's electronic spectrum simply by tuning the periodic potential. One of the simplest ways to apply a periodic potential is to use a superlattice potential, that is, a periodic potential induced by another crystal.[8]

Hexagonal boron nitride is a perfect candidate to make superlattices; its structure resembles that of graphene with boron and nitrogen atoms placed in a honeycomb lattice but is characterized by a constant lattice ∼1.8% larger than the one of graphene due to the longer B−N bond compared to the C−C. The superposition of graphene on h-BN in a random rotational orientation leads to the creation of a superlattice with a Moiré pattern whose wavelength (λ_M) and the lowest SDP energy (E_{SDP}) depend on the stacking angle (θ) between graphene and h-BN[6] as

$$\lambda_M = \frac{1.018 a_{CC}}{\sqrt{2.036[1 - \cos(\theta)] + 0.018^2}} \quad (1)$$

and

$$E_{SDP} = \frac{2\pi\hbar v_F}{\sqrt{3}\lambda_M} \quad (2)$$

where a_{CC} is the graphene lattice parameter and v_F is the Fermi velocity.[6] Equations 1 and 2 show that E_{SDP}, λ_M, and θ are all correlated to each other, so a graphene/h-BN superlattice can be described by only one of these parameters. From eqs 1 and 2, it follows that the longest Moiré wavelength (≃14 nm) is obtained for $\theta = 0$, that is, for a perfectly aligned graphene on h-BN. This sets E_{SDP} at ∼0.17 eV.

By using h-BN one can generate SDPs at a chosen energy,[2−7] which can allow designing of novel optical and opto-electronic devices with tunable properties. Consequently, it is vital to study the light interaction with h-BN/graphene superlattices.

Raman spectroscopy is a fast and nondestructive technique for investigating the properties of graphene,[9] which has already been shown to be sensitive to rotational faults in graphene-graphene stacks.[10−19] The Raman spectrum of twisted bilayer graphene (tBLG) shows some characteristic features: (i) peaks associated to phonon modes in the interior of the Brillouin zone can be activated by an umklapp double resonant Raman process in specific energy ranges.[13−15,18,19] (ii) A strong enhancement of the G peak intensity is observed for a twist angle between 10 and 15° at 633 nm excitation wavelength. This is caused by the presence of van Hove singularities in the

Received: July 19, 2013
Revised: October 24, 2013
Published: October 24, 2013

   dx.doi.org/10.1021/nl402679b | *Nano Lett.* 2013, 13, 5242−5246

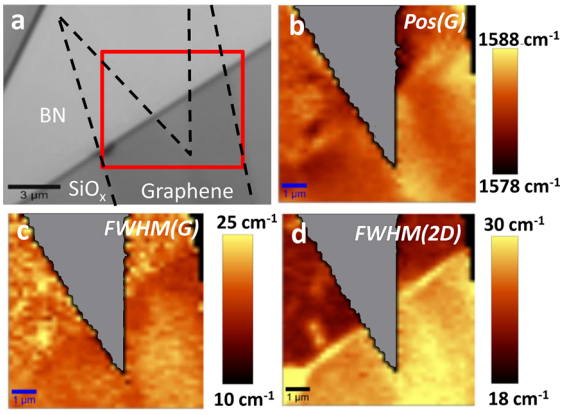

Figure 1. (a) Optical micrograph of a graphene flake transferred on a thick h-BN flake. (b) Raman map of the G peak position measured inside the red window shown in (a). (c) Raman map of fwhm(G) and (d) fwhm(2D) in the same area. The gray area in the Raman maps is not covered by graphene.

overlapping region of the Dirac cones of the top and bottom layer, which depend on the rotational angle between the two graphene.[16,17,19] (iii) The 2D peak shows a rather complex shape, depending on the excitation energy and mismatch angle because of the mutual interactions between the π/π^* bands associated to each graphene layer.[16,19]

Here we use Raman spectroscopy and transport measurements to study the changes in the Dirac spectrum of graphene/h-BN superlattices with the rotational angle. More than 30 graphene on h-BN structures with different degree of alignement have been investigated, following the fabrication process described in ref 7. Note that transport offers a straightforward way to probe SDPs because they appear as sharp peaks in resistivity.[7] From the position of the SDP in the resistivity plot, measured by transport, we extract the wavelength of the Moiré pattern and the rotational angle by using eqs 1 and 2 (more details in the Supporting Information, Figure S3). Transport measurements on these devices show charge carrier mobility of ~20−100 × 10^3 cm^2 V^{-1} s^{-1} and reduced charge inhomogeneity.[7] This rules out effects from doping and defects in our Raman spectra. Note that transport measurements using the electric field effect are limited to doping levels smaller than 10^{13} cm^{-2} (that is, energies <0.35 eV), which allows the observation of SDPs only in superlattices aligned with $\theta < 2°$.[7] Therefore, we define as "misaligned" all the structures with twist angle above 2°. A few tBLGs, produced by anodic bonding[20] were also investigated.

Figure 1a shows an optical micrograph of a graphene flake produced by micromechanical exfoliation and transferred onto a thick flake of h-BN placed on an oxidized Si wafer. The superlattice was made intentionally misaligned. Since graphene partially lies on the silicon substrate, we used this sample to investigate the dependence of the Raman spectrum on the substrate. Figure 1 shows the Raman map of (b) Pos(G); (c) fwhm(G); and (d) fwhm(2D), measured at an excitation energy of 2.41 eV. This figure shows that there is no appreciable difference in the G peak shape between h-BN and silicon. In the case of the 2D peak, significant differences can be observed: the 2D peak full width at hallf-maximum (fwhm) is larger on silicon (~30 cm^{-1}) than on h-BN (~21 cm^{-1}). An upshift in the 2D peak position of 9 cm^{-1} when graphene is deposited on h-BN, as compared to silicon, has also been observed. These results are in agreement with ref 21, which attributed the peak upshift to the partial removal of the Kohn-anomaly in the phonon dispersion near **K**, caused by the enhanced screening of the dielectric substrate. Note that exactly the same changes have been observed in tBLG for rotational angles >15° (see ref 16 and Supporting Information for measurements on tBLG, Figure S2).

Figure 2a plots the first order Raman spectrum measured at 2.41 eV on several devices with E_{SDP} varying from 0.17 eV (perfectly aligned) to above 0.35 eV (misaligned). The shape of the G peak strongly changes when moving from misaligned to aligned superlattices. The G peak of the misaligned device is a single and narrow peak lying at 1584 cm^{-1} and fwhm(G) = 10−13 cm^{-1}, similar to the G peak of suspended graphene.[22] Note that the peak marked with an asterisk in Figure 2 is an artifact, probably related to the substrate. In slightly misaligned structures, a weak and very sharp peak on the higher energy side of the G peak appears. Note that the position of this peak changes with the rotational angle and it is not dispersive, Figure 2a,b. Because of that, we attribute this peak to the intravalley umklapp activated R′ peak, associated to a LO phonon close to

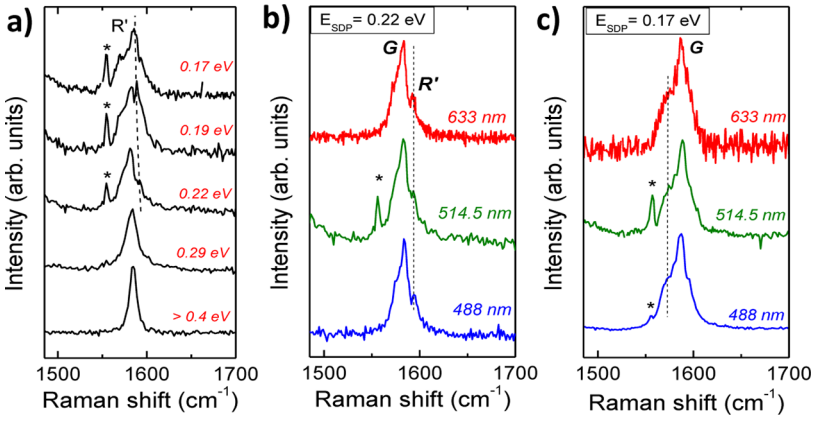

Figure 2. (a) G peak of graphene/h-BN superlattices measured at 2.41 eV as a function of E_{SDP} (b) and (c) multiwavelength analysis of the G peak of the superlattice with E_{SDP} = 0.22 eV and 0.17 eV, respectively. The peak marked with an asterisk is an artifact, probably related to the substrate. E_{SDP} has been measured by transport measurements (Figure S3 in the Supporting Information). The dashed lines in panels (a) and (b) are a guide to the eye and indicate the position of the R′ peak. The dashed line in panel (c) indicates the presence of a low energy shoulder at ~1570 cm^{-1} to the G peak.

dx.doi.org/10.1021/nl402679b | *Nano Lett.* 2013, 13, 5242−5246

the Γ point.[14] In order to confirm the origin of this peak, we determined the rotational wave-vector **G** characteristic of the h-BN/graphene superlattice by taking the difference between the reciprocal vectors of graphene and h-BN, starting from a perfectly aligned superlattice. We found

$$|\mathbf{G}| = \frac{4\pi\sqrt{2(1+\delta)(1-\cos\theta)+\delta^2}}{\sqrt{3}(1+\delta)a_{CC}} \quad (3)$$

where δ is the constant lattice mismatch (~1.8%). Assuming that the interaction between the two layers does not affect the phonon dispersion of graphene, we use the theoretical phonon frequencies of the monolayer from ref 23, and we obtain the frequency of the R′ peak as a function of the mismatch angle, Figure 3. Given the good agreement between measurements

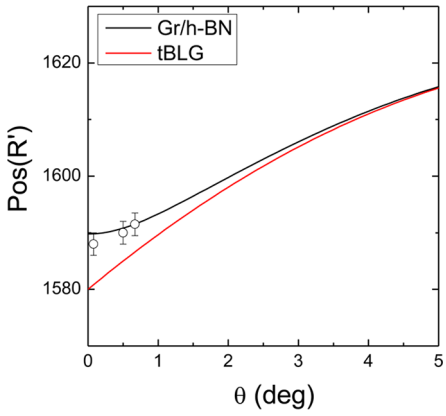

Figure 3. Plot of the R′ peak position as a function of θ for tBLG and h-BN/graphene superlattices. The dots are the experimental data obtained from the Raman spectra of aligned and slightly aligned h-BN/graphene superlattices. The error bar indicates the uncertainty in the Raman positions due to the resolution of the instrument (about 2 cm^{-1}).

and calculations (for the h-BN/graphene superlattice) further refinement of the theoretical model are beyond scope. Note that the R′ peak is not visible in perfectly aligned structures (θ = 0°), Figure 2c, since it overlaps with the G peak. For comparison, Figure 3 also shows the R′ dispersion calculated for the tBLG.[14] Differences between the tBLG dispersion and the graphene/h-BN one are visible only in the small twist angle regime (<2°) and are due to the different lattice mismatch in the two systems.

A careful analysis of the G peak shape in aligned structures also reveals that the G peak is asymmetric. By fitting the G peak with two lorenzians, the asymmetry is attributed to a peak centered at about 1570 cm^{-1} and fwhm of about 11−13 cm^{-1} (Supporting Information, Figure S4). Its position does not change significantly either with mismatch angle (<2°) or with excitation energy (Figure 2b,c). Since the intensity of this peak is rather weak, we used surface enhancement raman scattering (SERS) by depositing a thin gold film on the superlattice in order to increase the Raman signal of the aligned device (Supporting Information, Figure S7 shows the SERS spectra). We obtained an enhancement factor of 10−20 on the G peak. The SERS G peak is structured and in first approximation it can be fitted by two peaks centered at about 1570 and 1590 cm^{-1}, respectively (Supporting Information, Figure S7). The energy of the peak at 1570 cm^{-1} indicates that this is a TO phonon. This can become Raman-active in superlattices through intervalley resonant Raman scattering processes.[14,18] However, at small angles and small energies (~2 eV), the superlattice phonon wave-vector is too small to allow the intervalley Raman scattering process described in refs 14 and 18. Thus, the mechanism which activates the R peak in[14,18] cannot be used to explain the unusual line shape of the G peak of the aligned superlattices.

We now consider the second order Raman spectrum. Figure 4a shows the 2D peak measured at 1.96 eV on two superlattices

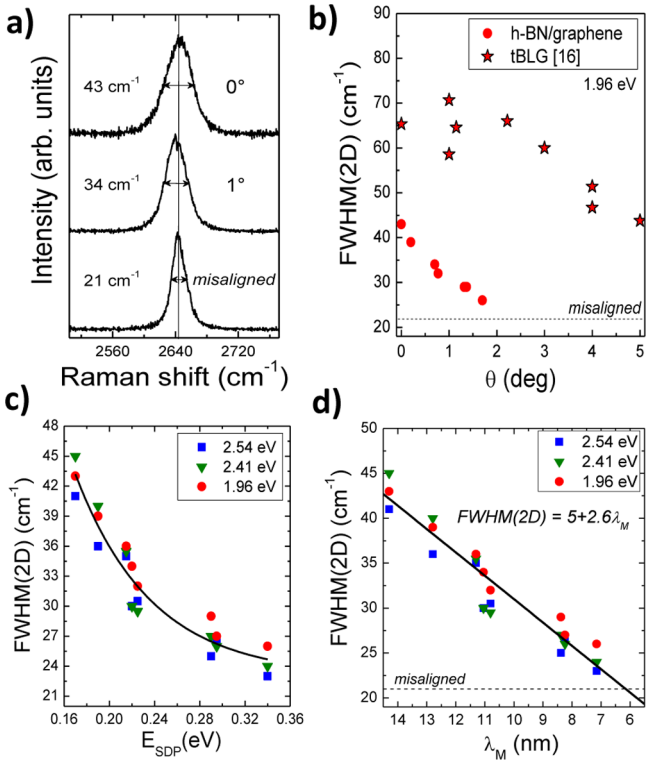

Figure 4. (a) Raman spectra taken at 1.96 eV on graphene deposited on BN with a mismatch angle of 0 and 1° as compared to a misaligned structure. (b) Experimental fwhm(2D) measured for graphene superlattice in ref 16 and h-BN/graphene structures (this work) at 1.96 eV. (c) Evolution of fwhm(2D) measured at a laser wavelength of 2.54, 2.41, and 1.96 eV as a function of superlattice Dirac point energy. (d) Linear dependence between fwhm(2D) and the Moiré wavelength. E_{SDP} has been measured by transport measurements (Figure S3 in the Supporting Information). Equations 1 and 2 have been used to calculate the Moiré wavelength and the mismatch angle from E_{SDP}.

with mismatch angles of 0 and 1° (top and middle spectra). These are compared with the 2D peak of a misaligned structure (bottom spectrum). This figure shows that the fwhm(2D) increases moving from a misaligned to a perfectly aligned superlattice. This is qualitatively similar to the behavior of tBLG, Figure 4b. Although at large angles the fwhm(2D) is the same for both superlattices (~21 cm^{-1}, Supporting Information, Figure S2), h-BN/graphene structures shows a much sharper increase in the fwhm(2D) at small angles, as compared to tBLG. The physics of the two systems (tBLG vs graphene/h-BN) is very different. Indeed, following ref 16, in tBLG the dependence of the 2D peak shape on the angle is due to the change in the electronic structure that is induced by the interaction between the two graphene layers. In particular, it stems from the mutual interaction between the π/π^* bands associated with the two distinct layers (see also ref 24). This

dx.doi.org/10.1021/nl402679b | Nano Lett. 2013, 13, 5242−5246

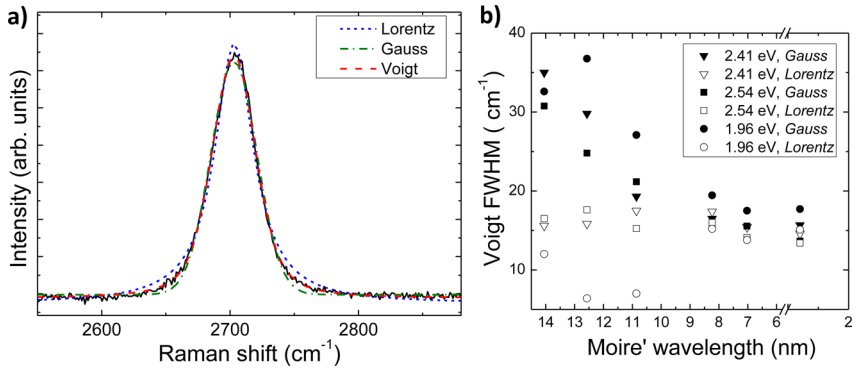

Figure 5. (a) Fitting of the 2D peak of an aligned h-BN/graphene superlattice. The best fit is obtained with a Voigt profile in which the width of both Gaussian and Lorentzian components are independent free parameters (Voigt). For comparison we also show the fit obtained with a purely Gaussian (Gauss) and a purely Lorentzian (Lorentz) line shape. (b) Parameters of the Voigt fit to the 2D peak as a function of the superlattice wavelength. For each fit, the two components (Gauss and Lorentz) of the Voigt profile are shown separately.

kind of mechanism cannot take place in the h-BN/graphene superlattice since there is only one graphene layer.

Figure 4c plots the fwhm(2D) measured at different excitation energies (1.96, 2.41, and 2.54 eV) for several devices against E_{SDP}. The characteristic broadening of the fwhm(2D) in aligned structures does not show any dependence with the excitation energy. Therefore, one can use this Raman fit parameter to identify aligned h-BN/graphene superlattices. In particular, a linear dependence is observed between fwhm(2D) and the Moiré wavelength for twist angles below 2°, Figure 4d. By fitting the data, we obtain fwhm$(2D) \simeq 5 + 2.6\lambda_M$. This equation offers a simple and fast way to determine the Moiré wavelength and E_{SDP} in slightly misaligned superlattices without using transport measurements or scanning tunneling microscopy.

Our results indicates that there are two very different regimes in graphene/h-BN superlattices. In misaligned structures, no difference between the fwhm(2D) of tBLG and h-BN/graphene superlattice is observed. Under this condition, there is no overlap between the Dirac cones of tBLG and the two layers are completely decoupled. This means that the top graphene is not "able to see" if the bottom layer is graphene or h-BN, so the Raman spectrum is expected to be qualitatively the same for the two superlattices. In slightly misaligned structures, h-BN/graphene superlattices show a characteristic sharp broadening of the 2D peak for decreasing mismatch angle. In particular, Figure 4d shows that this broadening appears for Moiré wavelength above 6 nm, corresponding to mismatch angles smaller than 2.5°.

Broadening of a Raman peak is typically attributed to defects.[27,28,25,26] However, this can be ruled out by both transport measurements[7] and by the Raman spectrum, which does not show any visible D peak. Note that identification of defects on graphene/h-BN superlattice could be difficult due to the intense BN Raman peak, which lies very close to the D peak. However, a strong broadening such as the one observed in this work would correspond to a very large amount of defects, giving $I(D)/I(G) > 3$.[27,28,25,26] Consequently, the D peak would be visible despite the BN peak. Therefore, the sharp increase of the fwhm(2D) must have a different origin.

The Raman spectrum is found to exhibit a simple and clear dependence to the misalignment between graphene and h-BN lattices. The broadening of the 2D peak can be caused by different effects. Let us start considering a change in the electron lifetime; this can happen only if the Moiré wavelength is comparable or smaller than the electron scattering length (about 5 nm at 2.4 eV[27]). In our case, however, the broadening is observed for Moiré wavelengths larger than 6 nm, so the electron−hole couple lifetime is not affected by the superlattice.

Besides, the 2D peak is double resonant and the broadening behavior can result from the interplay among different effects both in the electronic or in the phonon structure (see, for example, ref 23 and references therein). Taking into account that the 2D peak position does not strongly change with the Moiré wavelength, we can also assume the broadening behavior not to be caused by a change in the Kohn anomaly associated to the phonon dispersion at **K**.[23]

Therefore, one would be tempted to assign the 2D peak broadening to the reconstruction of the Dirac spectrum caused by the superlattice potential. This is an intrinsic effect, consequently it would not change the overall line shape of the 2D peak. However, by fitting the 2D peak with a Voigt function, we observe that the width of the Gaussian component strongly increases, while the width of the Lorentzian component remains constant, that is, the peak changes its shape from Lorentzian to Gaussian with increasing Moiré wavelength, Figure 5 (Supporting Information, Figure S8 shows the fit for misaligned and slightly misaligned structures). The increasing Gaussian character of the 2D peak let us to conclude that its broadening arises from an inhomogeneous distribution in the sample, which is characterized by the same spatial periodicity of the Moiré potential, being generated by the superlattice. This kind of periodic inhomogeneity may be originated by different effects, such as charge accumulation, strain, and so forth, and produces broadening of both the 2D peak and G peak (either as a splitting into the TO and LO components or as a distribution of different G peak associated to different area of the sample probed by the laser spot). This observation further indicates that the broadening is not related to the double-resonant Raman activation mechanism, which would affect only the 2D peak. Since doping level and local potential fluctuations are strongly suppressed when graphene is placed on h-BN,[21,29] our results indicate that a (spatial) periodic strain distribution in aligned superlattices is likely to be the origin of the changes observed in the Raman spectrum.

In conclusion, a characteristic broadening of the 2D peak of graphene/h-BN superlattices has been observed for mismatch angles below 2°. This allows high-throughput and non-destructive identification of aligned graphene/h-BN super-

dx.doi.org/10.1021/nl402679b | Nano Lett. 2013, 13, 5242−5246

lattices, making Raman spectroscopy a powerful tool in the fabrication of graphene superlattices based-devices.

■ ASSOCIATED CONTENT

Supporting Information

Details on the methods (Raman spectroscopy); the optical micrographs of the devices measured; the Raman maps of tBLG; resistivity measurements of the devices; fits of the G peak; multiwavelength analysis of the R′ peak; SERS spectra and fit of the corresponding G peak; 2D peak dispersion of aligned and misaligned structures; and Gaussian, Lorentzian and Voigt fits of the 2D peak for aligned and misaligned devices. This material is available free of charge via the Internet at http://pubs.acs.org.

■ AUTHOR INFORMATION

Corresponding Author

*E-mail: cinzia.casiraghi@manchester.ac.uk.

Notes

The authors declare no competing financial interest.

■ ACKNOWLEDGMENTS

C.C., A.K.G., and K.S.N. acknowledge useful discussions with M. I. Katsnelson. This work is partially funded by the Alexander von Humboldt Foundation in the framework of the Sofja Kovalevskaja Award, endowed by the Federal Ministry for Education and Research of Germany.

■ REFERENCES

(1) Kittel, C. In *Introduction to Solid State Physics*, 8th ed.; John Wiley and Sons: New York, 2004.

(2) Wallbank, J. R.; Patel, A. A.; Mucha-Kruczynski, M.; Geim, A. K.; Fal'ko, V. I. Generic Miniband Structure of Graphene on a Hexagonal Substrate. *Phys. Rev.* **2013**, *B87*, 245408.

(3) Park, C.-H.; Yang, L.; Son, Y.-W.; Cohen, M.; Louie, S. Anisotropic behaviours of massless Dirac fermions in graphene under periodic potentials. *Nature* **2008**, *4*, 213.

(4) Park, C.-H.; Yang, L.; Son, Y.-W.; Cohen, M.; Louie, S. New generation of massless Dirac fermions in graphene under external periodic potentials. *Phys. Rev. Lett.* **2008**, *101*, 14.

(5) Brey, L.; Feritg, H. A. Emerging Zero Modes for Graphene in a Periodic Potential. *Phys. Rev. Lett.* **2009**, *103*, 046809.

(6) Yankowitz, M.; Xue, J.; Cormode, D.; Sanchez-Yamagishi, J. D.; Watanabe, K.; Taniguchi, T.; Jarillo-Herrero, P.; Jacquod, P.; LeRoy, B. J. Emergence of superlattice Dirac points in graphene on hexagonal boron nitride. *Nat. Phys.* **2012**, *8*, 382.

(7) Ponomarenko, L. A.; Gorbachev, R. V.; Elias, D. C.; Yu, G. L.; Mayorov, A. S.; Wallbank, J.; Mucha-Kruczynski, M.; Patel, A.; Piot, B. A.; Potemski, M.; Grigorieva, I. V.; Novoselov, K. S.; Guinea, F.; Fal'ko, V. I.; Geim, A. K. Cloning of Dirac fermions in graphene superlattices. *Nature* **2013**, *497*, 594.

(8) Tsu, R. In *Superlattice to Nanoelectronics*, 2nd ed.; Elsevier Insights: New York, 2010.

(9) Casiraghi, C. *Raman spectroscopy of graphene, in Spectroscopic Properties of Inorganic and Organometallic Compounds: Techniques, Materials and Applications*; Yarwood, J., Douthwaite, R., Duckett, S., Eds.; The Royal Society of Chemistry: London, 2012; Vol.*43*, pp 29–56.

(10) Pocharal, P.; Ayari, A.; Michel, T.; Sauvajol, J. Raman spectra of misoriented bilayer graphene. *Phys. Rev. B* **2008**, *78*, 113407.

(11) Ni, Z.; Wang, Y.; Yu, T.; You, Y.; Shen, Z. Reduction of Fermi velocity in folded graphene observed by resonance Raman spectroscopy. *Phys. Rev. B* **2008**, *77*, 235403.

(12) Ni, Z.; Liu, L.; Wang, Y.; Shen, Z.; Li, L.-J.; Yu, T.; Shen, Z. G-band Raman double resonance in twisted bilayer graphene: Evidence of band splitting and folding. *Phys. Rev. B* **2009**, *80*, 125404.

(13) Gupta, A. K.; Tang, Y.; Crespi, V. H.; Eklund, P. C. Nondispersive Raman D band activated by well-ordered interlayer interactions in rotationally stacked bilayer graphene. *Phys. Rev. B* **2010**, *82*, 241406(R).

(14) Carozo, V.; Almeida, C. M.; Ferreira, E. H. M.; Canado, L. G.; Achete, C. A.; Jorio, A. Raman Signature of Graphene Superlattices. *Nano Lett.* **2011**, *11*, 4527.

(15) Campos-Delgado, J.; Cancado, L. G.; Achete, A. A.; Jorio, A.; Raskin, J.-P. Raman scattering studiy of the phonon dispersion in twisted bi-layer graphene. *Nano Res.* **2013**, *6*, 269.

(16) Kim, K.; Coh, S.; Tan, L. Z.; Regan, W.; Min Yuk, J.; Chatterjee, E.; Crommie, M. F.; Cohen, M. L.; Louie, S. G.; Zettl, A. Raman Spectroscopy Study of Rotated Double-Layer Graphene: Misorientation-Angle Dependence of Electronic Structure. *Phys. Rev. Lett.* **2012**, *108*, 246103.

(17) Havener, R. W.; Zhuang, H.; Brown, L.; Hennig, R. G.; Park, J. Angle-Resolved Raman Imaging of Interlayer Rotations and Interactions in Twisted Bilayer Graphene. *Nano Lett.* **2012**, *12*, 3162.

(18) Righi, A.; Costa, S. D.; Chacham, H.; Fantini, C.; Venezuela, P.; Magnuson, C.; Colombo, L.; Bacsa, W. S.; Ruoff, R. S.; Pimenta, M. A. Graphene Moiré patterns observed by umklapp double-resonance Raman scattering. *Phys. Rev. B* **2011**, *84*, 241409.

(19) Carozo, V.; Almeida, C. M.; Fragneaud, B.; Bede, P. M.; Moutinho, M. V. O.; Ribeiro-Soares, J.; Andrade, N. F.; Souza Filho, A. G.; Matos, M. J. S.; Wang, B.; Terrones, M.; Rodrigo B. Capaz, A.; Jorio, C. A.; Achete; Cancado, L. G. Resonance effects on the Raman spectra of graphene superlattices. *Phys. Rev. B* **2013**, *88*, 085401.

(20) Moldt, T.; Eckmann, A.; Klar, P.; Morozov, S. V; Zhukov, A. A.; Novoselov, K. S.; Casiraghi, C. High Yield Production and Transfer of Graphene Flakes Obtained by Anodic Bonding. *ACS Nano* **2011**, *5*, 7700.

(21) Forster, F.; Molina-Sanchez, A.; Engels, A.; Epping, S.; Watanabe, K.; Taniguchi, T.; Wirtz, L.; Stampfer, C. *Phys. Rev. B* **2013**, *88*, 085419.

(22) Berciaud, S.; Ryu, S.; Brus, L. E.; Heinz, T. F. Probing the Intrinsic Properties of Exfoliated Graphene: Raman Spectroscopy of Free-Standing Monolayers. *Nano Lett.* **2009**, *9*, 346.

(23) Venezuela, P.; Lazzeri, M.; Mauri, F. Theory of double-resonant Raman spectra in graphene: Intensity and line shape of defect-induced and two-phonon bands. *Phys. Rev. B* **2011**, *84*, 035433.

(24) Ferrari, A. C.; Meyer, J. C.; Scardaci, V.; Casiraghi, C.; Lazzeri, M.; Mauri, F.; Piscanec, S.; Jiang, D.; Novoselov, K. S.; Roth, S.; Geim, A. K. Raman Spectrum of Graphene and Graphene Layers. *Phys. Rev. Lett.* **2006**, *97*, 187401.

(25) Eckmann, A.; Felten, A.; Mishchenko, A.; Britnell, L.; Krupke, R.; Novoselov, K. S.; Casiraghi, C. Probing the Nature of Defects in Graphene by Raman Spectroscopy. *Nano Lett.* **2012**, *12*, 3925.

(26) Eckmann, A.; Felten, A.; Verzhibitskiy, I.; Davey, R.; Casiraghi, C. Raman study on defective graphene: Effect of the excitation energy, type, and amount of defects. *Phys. Rev. B* **2013**, *88*, 035426.

(27) Ferreira, E. H. M.; Moutinho, M. V. O.; Stavale, F.; Lucchese, M. M.; Capaz, R. B.; Achete, C. A.; Jorio, A. Evolution of the Raman spectra from single-, few-, and many-layer graphene with increasing disorder. *Phys. Rev. B* **2010**, *82*, 125429.

(28) Cancado, L. G.; Jorio, A.; Martins Ferreira, E. H.; Stavale, F.; Achete, C. A.; Capaz, R. B.; Moutinho, M. V. O.; Lombardo, A.; Kulmala, T. S.; Ferrari, A. C. Quantifying Defects in Graphene via Raman Spectroscopy at Different Excitation Energies. *Nano Lett.* **2011**, *11*, 3190.

(29) Dean, C. R.; Young, A. F.; Meric, I.; Lee, C.; Wang, L.; Sorgenfrei, S.; Watanabe, K.; Taniguchi, T.; Kim, P.; Shepard, K. L.; Hone, J. Boron nitride substrates for high-quality graphene electronics. *Nat. Nanotechnol.* **2010**, *5*, 5722.